Resonance Raman and Emission Investigation of the MLCT Transition in $Pt(PEt_3)_2(C{\equiv}CH)_2$

Chi Leung Choi, Yung Fong Cheng, Carol Yip, David Lee Phillips,* and Vivian Wing-Wah Yam*

Department of Chemistry, University of Hong Kong, Pokfulam Road, Hong Kong

Received February 14, 2000

Resonance Raman spectra including absolute Raman cross section measurements were acquired with excitation wavelengths within the MLCT absorption band of $[Pt(PEt_3)_2(C{\equiv}CH)_2]$. The absorption and resonance Raman cross sections were simultaneously modeled with time-dependent wave packet calculations to give an estimate of the vibrational reorganizational energies and initial structural changes of the excited state. We compare our results for $[Pt(PEt_3)_2(C{\equiv}CH)_2]$, which contains no phenyl groups, with previous results for $[Pt(dppm)_2(PhC{\equiv}C)_2]$, which contains a number of phenyl groups. The predominant nominal C≡C stretch reaction coordinate and the vibrational reorganizational energies are significantly altered in the initial excited state by the absence or presence of the aromatic substituents, and we semiquantitatively estimate these changes.

Introduction

The chemistry of metal acetylides has attracted enormous attention, in particular, with the emerging interest in their potential applications in the field of materials science. Metal acetylides have been increasingly employed as building blocks for molecular wires and organometallic oligomeric and polymeric materials which may possess unique properties such as optical nonlinearity, electrical conductivity, and liquid crystallinity. Recent work has shown that a number of metal acetylides also possess interesting and rich luminescence properties. Although there have been a number of investigations to elucidate the spectroscopy and photochemistry of metal acetylides,[1−12] relatively little is known about the structure of their excited states. Upon photoexcitation, some of these metal acetylides display photoluminescence and/or undergo photochemical reactions with other compounds via a somewhat long-lived excited electronic state.[1−12] Sometimes the structural changes associated with these photoexcitations can be deduced from vibronically resolved absorption and/or emission spectra.[13−16] However, there are many charge transfer absorption bands that do not display any vibronic structure (especially in room-temperature solutions where a lot of chemistry of interest takes place), and this makes it difficult to elucidate the structural changes of the excited state. Resonance Raman intensity analysis has been used by several groups[17−29] to determine the vibrational reorganizational energies or structural changes associated with the initial excited electronic state for diffuse absorption bands such as metal-to-ligand charge transfer (MLCT), ligand-to-ligand charge transfer (LLCT), intervalence transitions of inorganic complexes, organic noncovalent or covalent donor−acceptor compounds, and metal−metal charge transfer bands.

We have recently examined the MLCT transition (∼344 nm) of $[Pt(dppm)_2(PhC{\equiv}C)_2]$ using resonance

* Authors to whom correspondence should be addressed.

(1) Masai, H.; Sonogashi, K.; Hagihara, N. *Bull. Chem. Soc. Jpn.* **1971**, *44*, 2226.
(2) Sacksteder, L.-A.; Baralt, E.; DeGraff, B. A.; Lukehart, C. M.; Demas, J. N. *Inorg. Chem.* **1991**, *30*, 2468.
(3) Baralt, E.; Lukehart, C. M. *Inorg. Chem.* **1991**, *30*, 319.
(4) Stoner, T. C.; Geib, S. J.; Hopkins, M. D. *J. Am. Chem. Soc.* **1992**, *114*, 4201.
(5) Manna, J.; Geib, S. J.; Hopkins, M. D. *J. Am. Chem. Soc.* **1992**, *114*, 9199.
(6) Yip, H.-K.; Lin, H.-M.; Yang, Y.; Che, C. M. *J. Chem. Soc., Dalton Trans.* **1993**, 2939.
(7) Yam, V. W. W.; Chan, L.-P.; Lai, T. F. *Organometallics* **1993**, *12*, 2197.
(8) Yam, V. W. W.; Fung, W. K. M.; Cheung, K. K. *Angew. Chem., Int. Ed. Engl.* **1996**, 35, 1100.
(9) Yam, V. W. W.; Choi, S. W. K.; Cheung, K. K. *Organometallics* **1996**, *15*, 1734.
(10) Yam, V. W. W.; Chong, S. H. F.; Cheung, K. K. *Chem. Commun.* **1998**, 2121.
(11) Yam, V. W. W.; Lo, K. K. W.; Wong, K. M. C. *J. Organomet. Chem.* **1999**, 578, 3.
(12) Yam, V. W. W.; Yu K. L.; Cheung, K. K. *J. Chem. Soc., Dalton Trans.* **1999**, 2913.
(13) Clark, R. J. H.; Stewart, B. *J. Am. Chem. Soc.* **1981**, *103*, 6593.
(14) Clark, R. J. H.; Dines, T. J.; Doherty, J. M. *Inorg. Chem.* **1985**, *24*, 2088.
(15) Tutt, L.; Zink, J. I. *J. Am. Chem. Soc.* **1986**, *108*, 5830.
(16) Hanna, S. D.; Zink, J. I. *Inorg. Chem.* **1996**, 35, 297.
(17) Doorn, S. K.; Hupp, J. T. *J. Am. Chem. Soc.* **1989**, *111*, 1142.
(18) Doorn, S. K.; Hupp, J. T.; Porterfield, D. R.; Campion, A.; Chase, D. B. *J. Am. Chem. Soc.* **1990**, *112*, 4999.
(19) Wright, P. G.; Stein, P.; Burke, J. M.; Spiro, T. G. *J. Am. Chem. Soc.* **1979**, 101, 3531.
(20) Yang, Y. Y.; Zink, J. I. *J. Am. Chem. Soc.* **1984**, *106*, 1500.
(21) Wootton, J. L.; Zink, J. I. *J. Phys. Chem.* **1995**, *99*, 7251.
(22) Pedron, D.; Speghini, A.; Mulloni, V.; Bozio, R. *J. Chem. Phys.* **1995**, 103, 2795.
(23) Fraga, E.; Webb, M. A.; Loppnow, G. R. *J. Phys. Chem.* **1996**, *100*, 3278.
(24) Britt, B. M.; McHale, J. L.; Friedrich, D. M. *J. Phys. Chem.* **1995**, *99*, 6347.
(25) Markel, F.; Ferris, N. S.; Gould, I. R.; Myers, A. B. *J. Am. Chem. Soc.* **1992**, 114, 6208.
(26) Kulinowski, K.; Gould, I. R.; Ferris, N. S.; Myers, A. B. *J. Phys. Chem.* **1995**, *99*, 17715.
(27) Phillips, D. L.; Gould, I. R.; Verhoeven, J. W.; Tittlebach-Helmrich, D.; Myers, A. B. *Chem. Phys. Lett.* **1996**, 258, 87.
(28) Kwok, W. M.; Phillips, D. L.; Yeung, P. K.-Y.; Yam, V. W. W. *J. Phys. Chem. A* **1997**, 101, 9286.
(29) Leung, K. H.; Phillips, D. L.; Tse, M.-C.; Che, C.-M.; Miskowski, V. M. *J. Am. Chem. Soc.* **1999**, *121*, 4799.

10.1021/om000135d CCC: $19.00
Publication on Web 07/11/2000

Raman intensity analysis to estimate the structural changes of the initially excited ^{1}MLCT state and its short-time dynamics.[28] In this paper, we report a resonance Raman intensity analysis investigation of the $[Pt(PEt_3)_2(C{\equiv}CH)_2]$ (**1**) complex, which unlike the $[Pt(dppm)_2(PhC{\equiv}C)_2]$ (**2**) complex contains no phenyl groups. Comparison of results for **1** and **2** allows us to examine the extent of possible perturbation of the phenyl groups on the ^{1}MLCT transition of platinum acetylides, as well as the interplay of various kinds of excited states in governing the nature of the lowest-lying excited state upon a change in the acetylide orbital energy. We have also obtained a vibronically resolved room-temperature solution phase emission spectrum from the ^{3}MLCT state of **1**, and we use this to estimate the structural change in the ^{3}MLCT state. We discuss the ^{1}MLCT and ^{3}MLCT states' structural changes and their initial photophysics.

Experimental Section

$[Pt(PEt_3)_2(C{\equiv}CH)_2]$ (**1**) was prepared according to the literature method.[1] Sample solutions of **1** with concentrations of ~2 mM were prepared using spectroscopic grade dichloromethane solvent. The resonance Raman experimental apparatus and methods have been described previously[28,29] so only a short description will be presented here. The harmonics of a Nd:YAG laser and their hydrogen Raman shifted laser lines provided the excitation frequencies for the resonance Raman experiments. A stirred cell sample or flowing liquid jet sample was excited by a loosely focused laser beam, and a backscattering geometry was used to collect the Raman-scattered light with reflective optics. An ellipsoidal mirror imaged the Raman-scattered light through a depolarizer and entrance slit of a 0.5 m spectrograph onto a 1200 groove/mm grating, which dispersed the light onto a liquid nitrogen cooled CCD detector. The Raman signal was accumulated for 60−120 s by the CCD before being read out to an interfaced PC computer, and the addition of ~30−60 of these readouts were used to obtain the resonance Raman spectrum.

The known vibrational frequencies of the dichloromethane solvent Raman bands were used to calibrate the wavenumbers of the Raman spectra. Reabsorption of the Raman light by the sample was corrected for using previously described methods.[30] The spectra were also corrected for the wavelength variation of the detection system response using spectra of an intensity-calibrated tungsten lamp. An appropriately scaled solvent spectrum was subtracted from the sample resonance Raman spectra to remove solvent bands from the spectra. Portions of the spectra were fitted to a baseline plus a sum of Lorentzian bands in order to get the integrated areas of the Raman bands.

The concentrations of the sample solutions were determined spectrophotometrically before and after each absolute Raman cross section measurement, and changes of less than 5% were observed due to solvent evaporation and/or sample degradation. The sample absolute Raman cross sections were computed from the average of three trials at each excitation wavelength and measured relative to the known dichloromethane solvent Raman cross sections, which were previously measured relative to cyclohexane.[28] The maximum molar extinction coefficient for **1** was measured to be 7430 M^{-1} cm^{-1}. The phosphorescence spectrum of **1** was obtained using a SPEX Fluorolog-2 spectrofluorimeter.

Calculations

The computations presented here are not meant to be a complete description of the photoinduced charge transfer process in the Franck−Condon region of the MLCT transition of **1**, but are intended to give a reasonable estimate of the structural changes and short-time dynamics in the Franck−Condon region of the initial excited state. The absorption spectrum and resonance Raman intensities of **1** were simulated using a time-dependent methodology[31−34] and a simple model. The following equation was used to calculate the absorption spectrum:

$$\sigma_A(E_L) = (4\pi e^2 E_L M^2/3n\hbar^2 c) \int_{-\infty}^{\infty} d\delta\, G(\delta) \sum_i P_i \mathrm{Re}[\int_0^{\infty} \langle i|i(t)\rangle \exp[i(E_L + \epsilon_i)t/\hbar] \exp[-g(t)]\, dt] \quad (1)$$

and this expression was used to compute the resonance Raman cross sections:

$$\sigma_R(E_L,\omega_s) = \int_{-\infty}^{\infty} d\delta\, G(\delta) \sum_i \sum_f P_i\, \sigma_{R,i\to f}(E_L,\omega_s)\, \delta(E_L + \epsilon_i - E_S - \epsilon_f)$$

with

$$\sigma_{R,i\to f}(E_L,\omega_s) = (8\pi e^4 E_S 3E_L M^4/9\hbar^6 c^4) \left| \int_0^{\infty} \langle f|i(t)\rangle \exp[i(E_L + \epsilon_i)t/\hbar] \exp[-g(t)]\, dt\right|^2 \quad (2)$$

E_L is the incident photon energy, E_S is the scattered photon energy, and P_i is the initial Boltzmann population of the ground-state vibrational level $|i\rangle$ which has energy ϵ_i. M is the transition length (magnitude of transition dipole) evaluated at the equilibrium geometry, $G(\delta)$ is a Gaussian inhomogeneous distribution of electronic zero−zero frequency shifts centered at $\delta = 0$, and n is the refractive index of the solvent. $\delta(E_L + \epsilon_i - E_S - \epsilon_f)$ is a delta function to sum up cross sections with the same frequency. $|i(t)\rangle = e^{-iHt/\hbar}|i\rangle$, which is $|i(t)\rangle$ propagated on the excited-state surface for a time t, H is the excited-state vibrational Hamiltonian, f is the final state for the resonance Raman process, and ϵ_f is the energy of the ground-state vibrational level $|f\rangle$. The $\exp[-g(t)]$ part in eqs 1 and 2 is a damping function that depends on the nature of the electronic dephasing. In our system we chose to use a simple exponential decay function where $g(t)$ is given by

$$g(t) = t/\tau \quad (3)$$

Addition over a ground-state Boltzmann distribution of vibrational energy levels was used to calculate the absorption and resonance Raman cross sections. We used harmonic oscillators with their potential minima offset by Δ in dimensionless normal coordinates (the displacements are defined with respect to the ground-state frequency) to mimic the ground- and excited-state surfaces. The harmonic oscillators could have either the same frequencies or different frequencies as appropriate, and we assumed no coordinate dependence of the transition length (Condon approximation). Analytic

(30) Myers, A. B.; Li, B.; Ci, X. *J. Chem. Phys.* **1989**, 89, 1876.

(31) Myers, A. B.; Mathies, R. A. in Biological Applications of Raman Spectroscopy, edited by T. G. Spiro (Wiley: New York, 1987), Vol. 2, p 1.

(32) Clark, R. J. H.; Dines, T. J. *Angew. Chem., Int. Ed. Engl.* **1986**, *25*, 131.

(33) Zink, J. I.; Shin, K. S. K. *Adv. Photochem.* **1991**, 16, 119.

(34) Myers, A. B. *Acc. Chem. Res.* **1997**, *30*, 519.

expressions of Mukamel and co-workers[35] were used to numerically compute the time-dependent overlaps ($\langle i|i(t)\rangle$ and $\langle f|i(t)\rangle$) in eqs 1 and 2. The vibrational reorganizational energies, λ_v, were found from the dimensionless normal coordinates (Δ) by

$$\lambda_v = (\hbar\omega\Delta^2)/2 \quad \text{or} \quad \lambda_v = \hbar(\omega_e^2\Delta_g^2)/(2\omega_g) \qquad (4)$$

where $\hbar\omega$ is the vibrational frequency of the Franck–Condon active vibrational modes. The difference in the energy between the excited-state structure initially prepared at the reactant ground-state geometry and the relaxed equilibrium excited-state structure is termed the "reorganizational energy", λ. This "reorganizational energy" can be divided into contributions from the reacting molecule(s), which is called an internal reorganizational energy, and from the environment, a solvent reorganizational energy. The internal reorganization energy can be further divided into its contributions from individual vibrations, known as vibrational reorganizational energies.

The absorption spectrum and resonance Raman intensities are simultaneously modeled using eqs 1 and 2. Parameters such as the normal mode displacements (Δ) were adjusted to better fit the resonance Raman intensity pattern, and the transition length, E_0, and Δ_{max} were adjusted to better fit the integrated strength of the absorption spectrum, the position of its maximum, and its overall half-width. The solvent broadening contributions for inhomogeneous broadening ($G(\delta)$) and homogeneous broadening ($g(t)$) were adjusted to better fit the absolute Raman cross section and the absorption spectrum width. These parameters were adjusted iteratively until both the absorption spectrum, resonance Raman intensity pattern, and absolute resonance Raman cross sections were best fit with the simple model employed.

Results and Discussion

Figure 1 shows an absorption spectrum of **1** (top) and an overview of the 299.1 and 309.1 nm resonance Raman spectra (bottom) obtained in resonance with the absorption band at ~305 nm. The absorption band at ~305 nm has been tentatively assigned to a metal-to-ligand charge transfer (MLCT) transition.[1,2,6,7] The resonance Raman spectra in Figure 1 have been intensity corrected, solvent subtracted, and background subtracted. The resonance Raman spectra of **1** is similar to those previously reported for $Pt(dppm)_2(PhC{\equiv}C)_2$.[28] Most of the resonance Raman intensity appears in eight fundamental modes (409, 459, 566, 813, 978, 1039, 1223, and 1965 cm^{-1}) and several combination bands and an overtone band. The most intense band is the nominal C≡C stretch of the acetylide ligand, and this fundamental (1965 cm^{-1}) has an overtone (3950 cm^{-1}) and forms combination bands with the 409 and 459 cm^{-1} fundamentals (at 2379 and 2423 cm^{-1}, respectively).

Table 1 lists the Raman band wavenumbers and Raman cross sections for the 299.1 and 309.1 nm resonance Raman spectra of Figure 1. Table 2 gives the best fit parameters used to simulate the resonance Raman intensities and absorption spectrum of **1** using the simple model and computations described in the Calculations section. Figure 2 displays a graphical comparison of the calculated and experimental absorp-

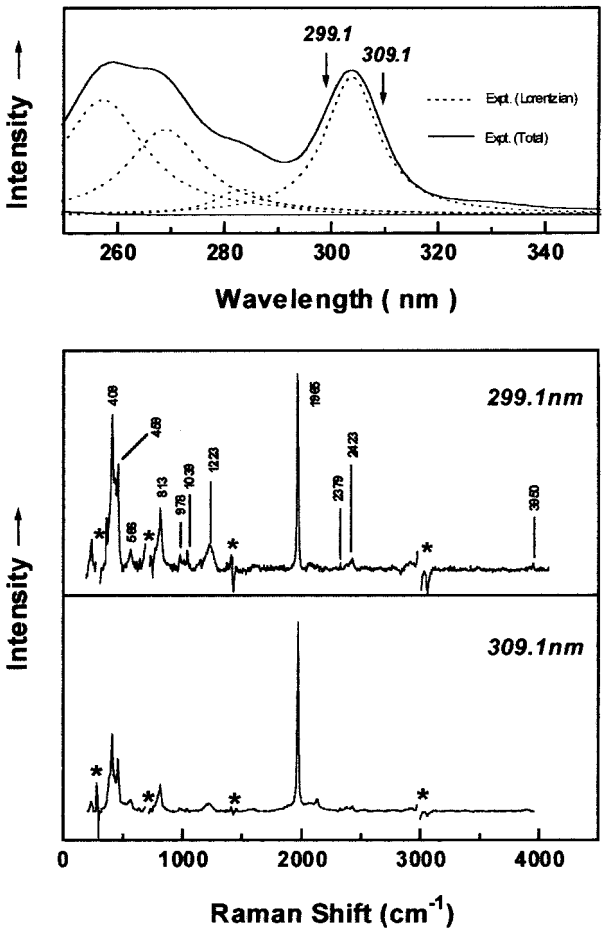

Figure 1. (Top) Electronic absorption spectrum of the $[Pt(PEt_3)_2(C{\equiv}CH)_2]$, **1**, complex in dichloromethane solution with the excitation wavelengths for the resonance Raman experiments indicated above the spectrum. The dashed lines show a Lorentzian deconvolution of the absorption spectrum. (Bottom) Overview of the 299.1 and 309.1 nm resonance Raman spectra of **1**. The spectra have been intensity corrected, solvent subtracted, and background subtracted. The asterisks (*) mark regions where solvent subtraction artifacts are present.

Table 1. Resonance Raman Bands of $[Pt(PEt_3)_2(C{\equiv}CH)_2]$ (1) in Dichloromethane Solution (Raman Shifts and Absolute Raman Cross Sections)

peak	Raman shift[a] (cm^{-1})	299.1 nm[c] expt[b]	299.1 nm[c] calc	309.1 nm[c] expt[b]	309.1 nm[c] calcd
fundamental	409	2.91	2.68	0.74	0.72
fundamental	459	1.05	1.32	0.28	0.31
fundamental	566	0.49	0.37	0.09	0.07
fundamental	813	1.72	1.66	0.32	0.25
fundamental	978	0.36	0.23	0.03	0.04
fundamental	1039	0.15	0.08	0.016	0.014
fundamental	1223	1.48	1.15	0.19	0.23
fundamental	1965	1.9	2.78	0.79	0.89
combination (1965+409)	2379	0.11	0.12	0.02	0.02
combination (1965+459)	2423	0.10	0.06	0.03	0.01
overtone (2 × 1965)	3950	0.07	0.06	0.019	0.014

[a] Estimated uncertainties are about 4 cm^{-1} for the Raman shifts. [b] Estimated uncertainties are about 10% for intensities 1.0 × 10^{-9} $Å^2$/molecule and higher, 20% for intensities between 0.1 and 1.0 × 10^{-9} $Å^2$/molecule, and 50% for intensities lower than 0.10 × 10^{-9} $Å^2$/molecule. [c] × 10^{-9} $Å^2$/molecule.

(35) Yan, Y. J.; Mukamel, S. *J. Chem. Phys.* **1987**, 86, 6085.

Table 2. Parameters for Calculation of Resonance Raman Intensities of $[Pt(PEt_3)_2(C{\equiv}CH)_2]$ (1)[a]

ground-state vibrational wavenumber/cm^{-1}	excited-state wavenumber/cm^{-1}	$\|\Delta\|$	vibrational reorganizational wavenumber/cm^{-1}
409	409	0.45	41
459	459	0.29	19
566	566	0.12	4
813	813	0.195	15
978	978	0.07	2
1039	1039	0.042	1
1223	1223	0.16	15
1965	1965	0.285	80
			total $\lambda_v = 177$

[a] Transition length, $M = 0.45$ Å, $E_0 = 32\ 850$ cm^{-1}, $n = 1.45$. Homogeneous broadening, $\Gamma = 460$ cm^{-1} hwhm. Inhomogeneous broadening, $G = 50$ cm^{-1} standard deviation.

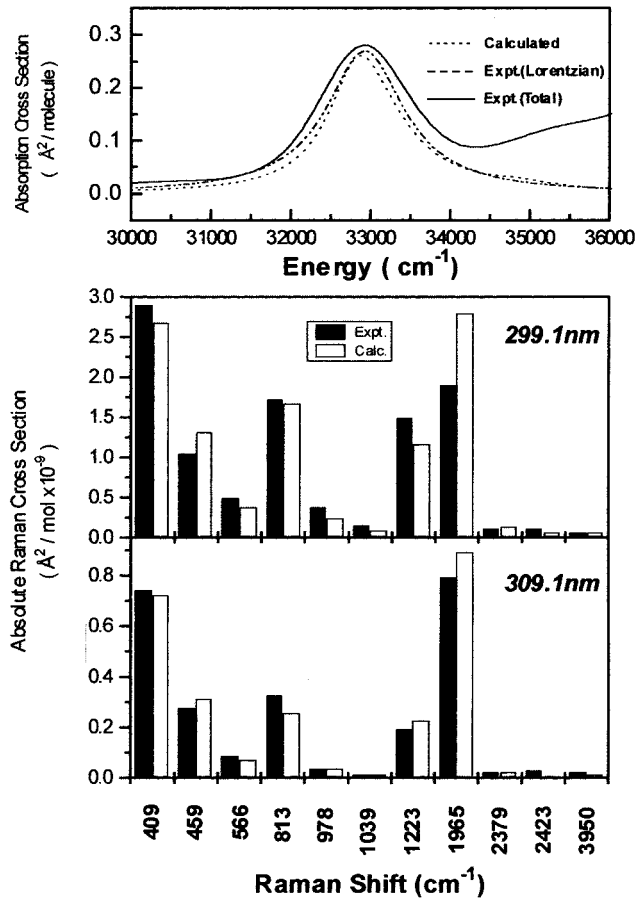

Figure 2. (Top) Comparison of the calculated (dotted line), Lorentzian deconvolution (dashed line), and experimental (solid line) electronic absorption spectra of **1**. The best fit parameters of Table 2 in eq 1 and the simple model described in the Calculations section were used to obtain the calculated absorption spectrum. (Bottom) Comparison of the calculated (open bars) and experimental (solid bars) resonance Raman cross sections for the 299.1 and 309.1 nm resonance Raman spectra of **1**. The parameters of Table 2 in eq 2 and the simple model given in the Calculations section were used to obtain the calculated Raman cross sections.

tion and resonance Raman cross sections for **1**, and Table 1 presents a tabular comparison of the experimental and calculated Raman cross section. There is reasonable agreement between both the absorption and resonance Raman calculated and experimental cross sections. Most of the initial excited-state vibrational

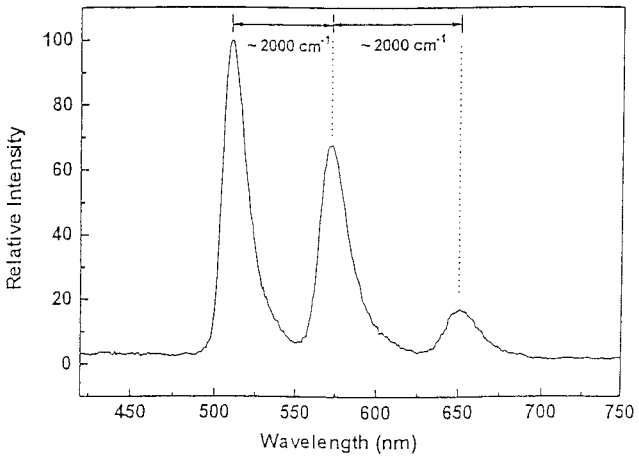

Figure 3. Emission spectrum of **1** in degassed dichloromethane solution at 298 K.

reorganizational energy and displacement is along the nominal C≡C stretch, and this is consistent with the assignment of the absorption band to a MLCT transition from the Pt to an acetylide ligand. If we assume that the nominal C≡C stretch mode can be approximated by a pure C≡C stretch, then we can estimate the bond length change along this coordinate in the initial excited state by using

$$q = (\mu\omega/\hbar)^{1/2}(\Delta x) \qquad (5)$$

where q is the dimensionless normal coordinate, μ is the reduced mass of the C≡C bond, ω is the ground-state vibrational frequency, and Δx is the change in the bond length. Using the parameters for **1** in Table 2, we find that the excited-state bond length change is ~0.04 Å. We have also acquired the emission spectrum of the ^{3}MLCT state, and this is shown in Figure 3. This spectrum in Figure 3 displays mainly a progression with ~2000 cm^{-1} spacing, and this suggests that the phosphorescent triplet MLCT state exhibits a noticeable structural change along the nominal C≡C stretch mode for **1**. A simple estimate of the C≡C bond length change in the phosphorescent triplet state can be found using the spectrum of Figure 3 and the following formula:

$$\Delta x = [2S\hbar\omega_g/\mu\omega_e^2]^{1/2} \qquad (6)$$

where Δx is the bond length change, μ is the reduced mass of the bond, and S is the ratio of the vibronic (1,0) and (0,0) intensities, which is the Huang−Rhys factor. Using $\omega_g = 1965$ cm^{-1} and $\omega_e = 1800$ cm^{-1}, this gives a bond length change of ~0.09 Å for the C≡C bond in the ^{3}MLCT phosphorescent state. This indicates that the initial MLCT state has only a partial change or weakening of the C≡C bond by ~0.04 Å relative to the ground state, and then this further weakens in the triplet MLCT state by ~0.09 Å relative to the ground state.

It is interesting to compare our present results for **1** with those previously found for $Pt(dppm)_2(PhC{\equiv}C)_2$, **2**, which contains a number of phenyl groups.[27] Comparison of the MLCT resonance Raman spectra of **1** with **2** shows that the spectra of **2** have more intensity in the overtones and combination bands of the main C≡C stretch mode. This is consistent with the larger dimensionless normal mode displacement parameter found

from the simulations for the C≡C stretch mode in **2** (Δ = 0.620 from ref 28) compared to **1** (Δ = 0.285). Assuming that the nominal C≡C stretch mode is a pure stretch, we can use eq 5 to estimate C≡C bond length changes of ~0.04 Å for **1** and ~0.09 Å for **2** for the initial excited state. This suggests that the aromatic groups in **2** significantly perturb the C≡C reaction coordinate. The total vibrational reorganizational energy found for **2** (~563 cm^{-1} from ref 28) is also significantly larger than that for **1** (~177 cm^{-1}), and the distribution of energy between the predominant C≡C stretch mode and the other modes also appears to shift noticeably (80 cm^{-1} out of 177 cm^{-1} for **1** compared to 406 cm^{-1} out of 563 cm^{-1} for **2**). The best fit simulation parameters for **1** and **2** also have large changes in the amount of homogeneous and inhomogeneous broadening needed to simultaneously fit the absolute Raman cross sections and absorption band: the homogeneous broadening parameter was 460 cm^{-1} for **1** and 100 cm^{-1} plus a lifetime broadening of 45 cm^{-1} for **2** (hwhm), while the inhomogeneous broadening parameters were about 50 cm^{-1} for **1** and 690 cm^{-1} for **2** (standard deviation). The aromatic substituents of compound **2** appear to noticeably perturb the Pt to acetylide MLCT transition of **1** by drawing the charge and associated structural changes further out into the ligands. This seems to be consistent with the changes observed in the total vibrational reorganizational energy (from 177 cm^{-1} in **1** to 563 cm^{-1} in **2**) as well as the proportionately larger amount of change in the C≡C stretch compared to the lower frequency 409 and 459 cm^{-1} modes associated with the Pt−P and Pt−C groups for **2** compared with **1**. Since the acceptor π^* acetylide orbitals are higher in energy in **1** than **2** (π^* orbital energy: −C≡CH > −C≡CPh) and closer to the 3d orbital of phosphorus (P), we would expect the MLCT transition of **1** to have somewhat more Pt−P character. Comparison of the MLCT resonance Raman spectra and best fit simulation parameters for **1** with those for **2** does indicate there is more enhancement of the Pt−P modes ~400−460 cm^{-1} relative to the predominant nominal C≡C stretch in **1** compared with **2**.

Typical bond lengths for C≡C and C═C are 1.204 ± 0.002 and 1.337 ± 0.006 Å, respectively (from 62nd edition of the CRC Handbook of Physics and Chemistry). This gives a bond length change of about 0.133 Å for a full bond order change of the carbon−carbon bond from C≡C to C═C. We find bond length changes of around 0.04−0.09 Å for the acetylide in **1** and **2** upon excitation of the MLCT transition (~305 nm for **1** and ~344 nm for **2**), and these changes appear to be consistent with an expected nominal change of bond order from 3 to 2.5 for an electron transfer from Pt to a π^* orbital of the acetylide. Such bond order changes, together with the observed Huang−Rhys factor $S < 1$, are further supportive of an assignment of a MLCT nature rather than that of an intraligand $\pi-\pi^*$ transition. Our results for **1** and **2** suggest that the initial MLCT state reaction coordinate and structural changes are noticeably influenced by aromatic substituents possibly through some π orbital interaction with the acetylide ligand as well as the relative energy separation of the acceptor π^* acetylide orbital with the 3d P orbital.

Acknowledgment. This work was supported by grants from the Committee on Research and Conference Grants (CRCG), the Research Grants Council (RGC) of Hong Kong, the Hung Hing Ying Physical Sciences Research Fund, and the Large Items of Equipment Allocation 1993−94 from The University of Hong Kong.

OM000135D